THE AD 1881 EARTHQUAKE-TRIGGERED SLUMP AND LATE HOLOCENE FLOOD-INDUCED TURBIDITES FROM PROGLACIAL LAKE BRAMANT, WESTERN FRENCH ALPS

H. GUYARD [a, b], G. ST-ONGE [a, b], E. CHAPRON [c], F. S. ANSELMETTI [c], P. FRANCUS [d, b]

[a.] *Institut des Sciences de la Mer (ISMER) à Rimouski, Université du Québec à Rimouski, 310 allée des Ursulines, Rimouski, Québec, Canada, G5L3AI*

[b.] *GEOTOP-UQAM-McGill, C.P. 8888, Succursale Centre-ville, Montréal, Québec, Canada, H3C 3P8*

[c.] *Geological Institute ETH Zürich, Universitätstrasse 16, CH-8092 Zürich, Switzerland*

[d.] *Institut National de la Recherche Scientifique- Eau, Terre, et Environnement (INRS-ETE), 490 de la Couronne, Québec, Québec Canada, G1K 9A9*

Abstract

High-resolution seismic analyses on the sedimentary subsurface of the deep basin of proglacial Lake Bramant (Grandes Rousses Massif, Western French Alps) allowed the detection of a large lens-shaped body with chaotic internal reflections corresponding to a mass wasting deposit (MWD) triggered by the nearby AD 1881 Allemond earthquake (MSK intensity VII). This MWD was only retrieved at the base of a short gravity core and the top of a piston core. Sediments associated with this MWD are remoulded and laminated. Locally, blocks of sediment have preserved the original stratification. This earthquake-induced mass movement is an example of a slide that evolved into a slump. In addition, several Late Holocene turbidite and hyperpycnal deposits related to exceptional flood events were identified using high-resolution sedimentological, physical and geochemical analyses. However, the identification of hyperpycnites is sometimes complicated as erosion of the basal sequence can occur during the rising limb of the flood. While the precise dating of the oldest flood event is still ongoing, two flood events are coeval with the St. Sorlin glacier retreat following the end of the "Little Ice Age", suggesting outbursts of temporary ice contact lakes or subglacial lakes during warmer periods.

Keywords: slump, earthquake, hyperpycnites, turbidites, floods, proglacial lake, Western French Alps

1. Introduction

In lacustrine systems, mass wasting deposits such as slumps or turbidites can be generated by processes such as lake level change or slope overloading, but are more often triggered by the regional seismo-tectonic activity (Sims, 1975; Doig, 1986), especially in the Alpine region (Chapron et al., 1999; Schnellmann et al., 2002; Monecke et al., 2004; Nomade et al., 2005; Strasser et al., 2006). In addition, several major historic floods were previously recorded

in Alpine lake sediments and were associated with hyperpycnal flows (Arnaud et al., 2002; Schneider et al., 2004). Hyperpycnal deposits (hyperpycnites) are characterized by the development of a coarsening-up basal unit during the increasing discharge period (up to the peak of the flood) and by a fining upward top unit during the decreasing discharge period (from the peak of the flood) (Mulder et al., 2001a, 2003; St-Onge et al., 2004; Chapron et al., 2006; St-Onge and Lajeunesse, this book). In proglacial environments, they can be deposited after the catastrophic drainage (i.e outburst) of a subglacial lake. Traditionally, the identification of catastrophic events resulting in mass movements such as earthquakes or exceptional floods is based on a range of sedimentological and textural criteria from visual description of sedimentary structures, on grain size measurements and on the establishment of a precise chronology. In this paper, we use a high-resolution multiproxy approach to identify, detail and determine the trigger mechanism of several rapidly deposited layers recorded in the deep basin of proglacial Lake Bramant in the Grandes Rousses Massif, Western French Alps (Fig. 1).

2. Setting

The Grandes Rousses Massif is affected by large tectonic features such as basement thrusts and strike-slip faults. The study area has been historically subjected to several moderate magnitude earthquakes (Chapron et al., 1999; Nomade et al., 2005) (Fig. 1a). Among them, the AD 1881 Allemond earthquake (intensity MSK VII) had an epicenter located less than 12 km away from Lake Bramant.

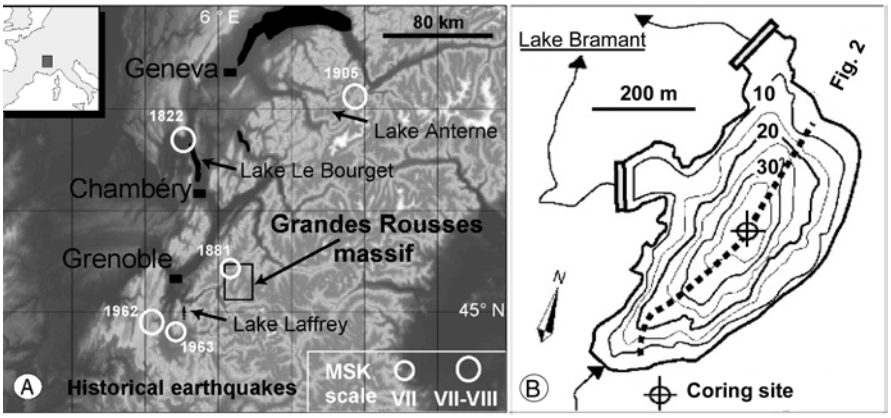

Figure 1: (A) General location of the Grandes Rousses Massif in the Western French Alps. Also shown are the MSK intensities at the epicentres of regional historical earthquakes previously recorded in lake sediments. (B) Bathymetry of Lake Bramant (thick isobaths: 5 m), situated on the northern part of the Massif. Hydroelectric dams were built at the lake outlets in 1918. Location of the coring site is based on seismic reflection profiling. The location of the seismic profile shown in Figure 2 is indicated by a thick dotted line.

This lake is situated at 2448 m a.s.l, is 600 m long, 400 m wide and has a maximum depth of ~39 m (Fig. 1b). It is the lowermost lake of a chain of three

small proglacial lakes of the St-Sorlin glacier which is situated on the northern part of the Grandes Rousses Massif (see Guyard et al., subm. for details). In addition, temporary ice-marginal lakes are frequently observed at the margin of the St. Sorlin glacier (M. Vallon, pers. comm.) and subglacial lakes may have also formed in the past below the St. Sorlin glacier.

3. Methods

3.1 Coring site

The sedimentary infill of Lake Bramant was imaged with the ETH Zurich 3.5 kHz pinger system. Conventional GPS navigation allowed the acquisition of a dense grid of high-resolution seismic profiles with a mean line spacing ranging between 50 and 100 m (Fig. 2).

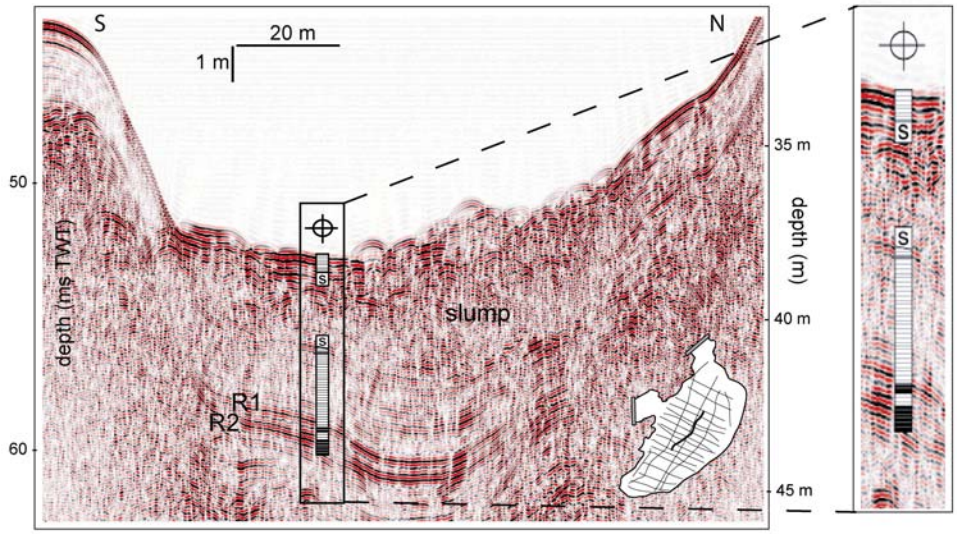

Figure 2: Seismic profile (3.5 kHz) across Lake Bramant deep basin and enlarged section illustrating the stratigraphy at the coring site. Undisturbed sediments were retrieved above and below a large mass wasting deposit (MWD) highly deformed as discussed in the text. This slump (S) and two high-amplitude reflections (R1 and R2) are clearly visible in the deepest and thickest part of the basin (see Guyard et al., subm. for details).

The system imaged an up to 20 ms two-way travel time (TWT) thick sedimentary succession and allowed the selection of a coring site in the depocenter of the basin. Following the seismic survey, a short gravity core (BRA03-1, 80 cm-long) and a long piston core (BRA03, cored interval 190-510 cm below lake floor) were taken in order to retrieve the best-possible undisturbed sediments above and below a large lens-shaped body with low-amplitude chaotic internal reflections that covers most of the deep basin and is the thinnest at the coring site (Fig. 2). This typical acoustic facies indicating mass wasting deposits (MWD) was only retrieved at the base of the short gravity core and the top of the piston core (Fig. 2 and 3), confirming the seismic interpretation that the non-cored interval (80-190 cm) only consists of MWD deposits. The absolute depth of the piston core was determined by core-to-seismic correlation.

3.2 Multiproxy sediment core analyses

Cores were split, described and photographed with a 400 d.p.i. resolution digital camera, before u-channels were sampled in the middle of the cores in order to study geochemical and physical properties at very high resolution in undisturbed sediments. CAT-Scan (computerized axial tomography) analyses were carried out at INRS-ETE (Québec City) with a pixel resolution of 1 mm for the extraction of CT number profiles. The CT number primarily reflects bulk density variations (St-Onge et al., 2007). Micro-fluorescence-X (XRF) analyses were performed with an ITRAX core scanner (Croudace et al., 2006) with a downcore resolution of 300 µm for BRA03-1 and 100 µm for BRA03. BRA03-1 was irradiated during 1 s whereas BRA03 was irradiated during 10 s. The radiographs obtained were transformed in negative X-ray images. Finally, in short core BRA03-1 and piston core BRA03, sediment grain size distribution was determined at ISMER (Rimouski) using a Beckman-Coulter LS-13320 (0.04 to 2000 µm) laser sizer with a sampling interval ranging from 0.5 to 1 cm in the rapidly deposited layers. Data was processed with Gradistat software (Blott and Pye, 2001).

4. Results and discussion

4.1 AD 1881 Earthquake-triggered slump.

Based on varve counting, the top of the MWD affecting most of the deep basin (Fig. 2) is dated at AD 1886 ± 5 and can thus be associated to the nearby AD 1881 Allemond earthquake (Fig. 1) (Guyard et al., subm.). In addition, this type of mass movements creates failure scars on the subaqueous slopes. Such scars were detected just below the lake floor and suggest thus that unstable sediments were remobilized by earthquake ground accelerations in various simultaneous mass flows, a criteria used previously to single out earthquake shaking as trigger mechanism (Schnellmann et al., 2002). The base of the MWD is observed at 217 cm, just above deformed laminae deposited during a normal sedimentation period (Fig. 3). The deformed background sediments likely result from the rapid deposition of an important quantity of sediments (1.10 m at the coring site). Sediments incorporated in the slump have a lighter colour with regards to the rest of the core and are remoulded, laminated and highly deformed in specific intervals. The base of core BRA03-1 shows that the MWD is composed of locally folded and remoulded sediments and of reworked sediment blocks with their original laminations as seen on the Rx images. In addition, a homogenous layer is observed at the base of BRA03-1 at 80-71 cm, whereas a sand layer is recorded at 65-68 cm. The mechanism responsible for the deposit of the sediments between 46-217 cm thus involved unequivocally a mass wasting event. This earthquake-induced mass movement is an example of a rotational sediment slide (Locat & Lee, 2002), corresponding to a slump following the classification of Mulder & Cochonat

(1996). Moreover, the skewness *vs.* sorting diagram (Fig. 3b) does not illustrate a specific energy evolution such as for a classical turbidite or for a hyperpycnal deposit (see fig. 4), indicating a slumping mechanism.

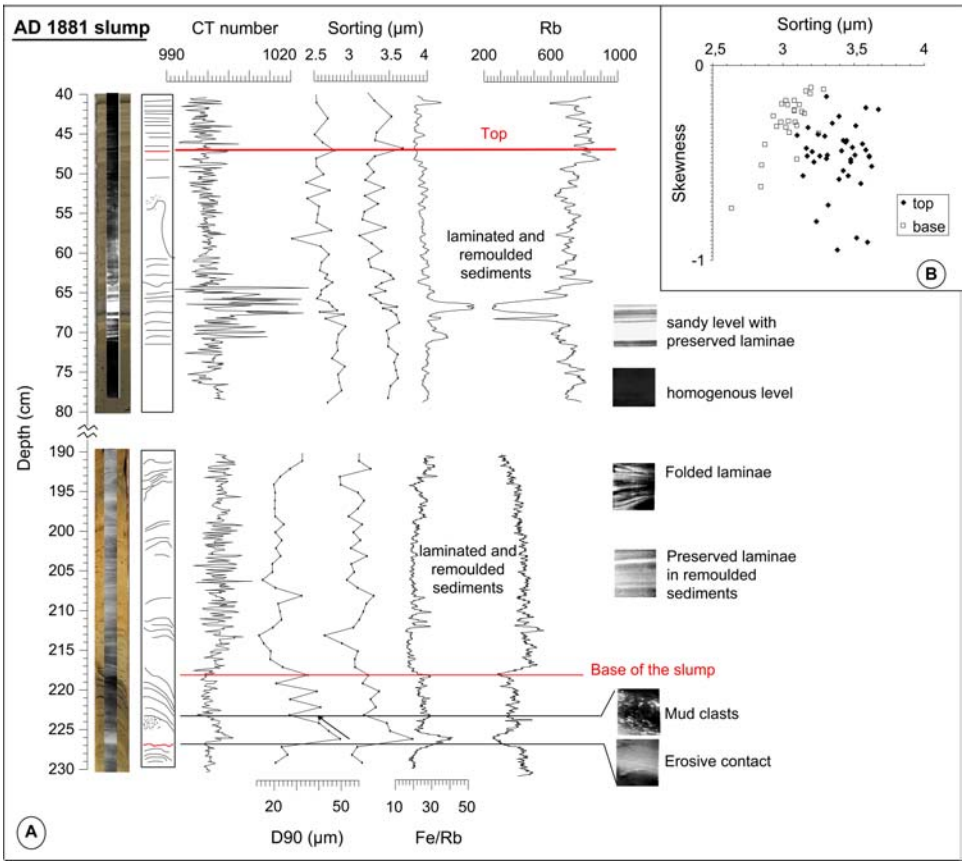

Figure 3: (A) Physical, sedimentological and geochemical properties of the base (190-217 cm) and the top (46-80 cm) of the slump triggered by the AD 1881 Allemond earthquake (MSK VII). Digital photographs, Rx images and chemical composition are obtained from the ITRAX measurements; VFSa: very fine sand percent (from 63 to 125 µm). The interval between 80-190 cm was not retrieved due to coring strategy. Just below the slump, an incomplete Bouma turbidite sequence is deposited. (B) Skewness *vs*. sorting diagram for the slump deposit.

Below the slump, a fining upward sequence beginning with an erosive contact is detected between 227-223 cm (Fig. 3) just above a thin olive-green layer, likely corresponding to the past sediment/water interface that was rapidly recovered by an instantaneous deposit. Coarser sediments at the base of this sequence are also indicated by the higher CT number values and the lighter X-ray grey scale, whereas mud clasts are observed on the Rx images from 226 to 224 cm. In addition, the observed increase in Fe and decrease in Rb contents within that interval are also suggesting a coarser base. Indeed, a Fe enrichment was previously interpreted as an indicator of the base of turbidites, whereas variations of the Rb content were related to fluctuations in the amount of detrital clays (Rothwell et al., 2006). Similarly, Fe in Lake Bramant sediments is concentrated in the coarse fraction especially at the base of turbidites,

whereas Rb reflects the finer sediment fluctuations associated with the "glacial flour" resulting from glacial erosion. Based on this sharp contact, the normal grading and the presence of mud clasts, this sequence likely corresponds to an incomplete Bouma turbidite (e.g., Bouma, 1962; Mulder et al., 2001b), where only facies Ta-Tb were recorded. This turbidite could have been triggered by an earthquake, but could have also been generated by a storm event or an exceptional flood.

4.2 Flood-induced turbidites

Rapidly deposited layers, labelled E2 and E3, are also recorded at 25-28 cm and 31-35 cm, respectively (Fig 4).

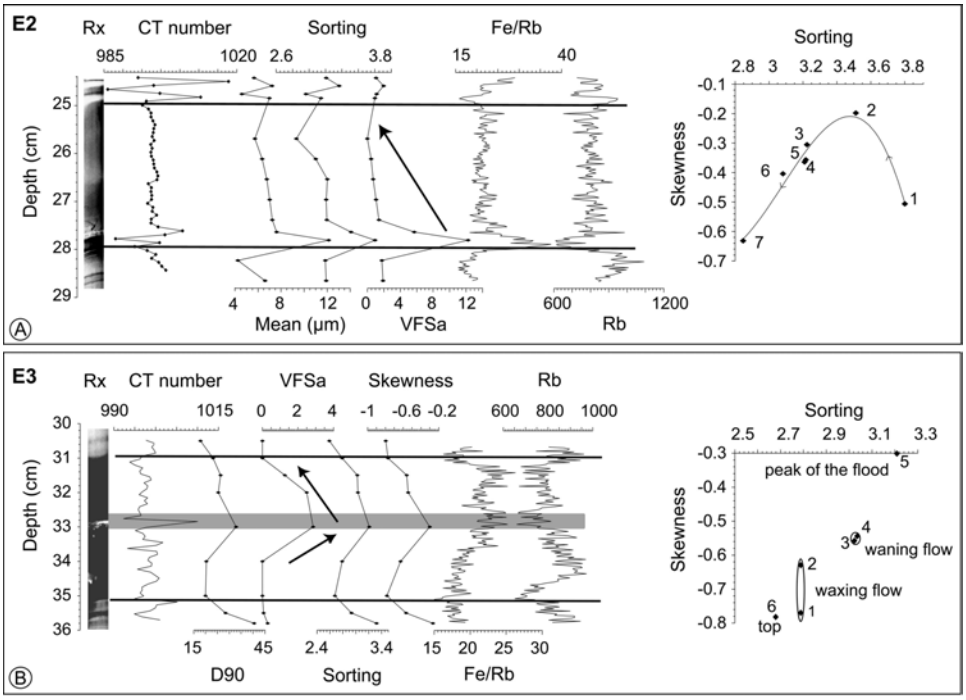

Figure 4: Physical, sedimentological and geochemical properties of sedimentary events E2 (A) and E3 (B). Rx images are obtained from the ITRAX measurements; VFSa: very fine sand percent (from 63 to 125 µm). Skewness *vs.* sorting diagrams for both layers are also displayed.

In the 4 cm-thick sedimentary event E3 (Fig. 4b), the basal sequence is characterized by an inverse grading (coarsening upward). The middle of the deposit (around 33 cm) is characterized by a thin layer of very fine sand, notably highlighted by a lighter grey scale and by a peak in the CT number, indicating a higher bulk density. Above the sand layer, the different proxies are reflecting a normal grading (fining upward). This grain size evolution is typical of hyperpycnal flows generated by large flood events in marine or lacustrine environments (e.g., Mulder et al., 2001a; 2003; St Onge et al., 2004; Schneider et al., 2004; Chapron et al., 2006; St-Onge and Lajeunesse, this book). The waxing flow (rising limb

of the flood) results in the development of the inversely graded bed up to the peak of the flood, whereas the waning flow (falling limb of the flood) results in the subsequent normal grading. This hyperpycnal sequence is also reflected in the skewness *vs.* sorting diagram, where higher values of skewness and sorting indicate stronger energy and turbulence during the waxing flow and lower values of skewness and sorting argue for gradually decreasing energy during the waning flow. The distribution of very fine sands and evolution of mean grain size in the 4 cm-thick sedimentary event E2 (Fig. 4a) depict the development of a normally-graded sequence starting with a coarse base sharply fining upward. The representative points in the sorting vs skewness diagram are indicative of a sequence deposited in an environment with a gradually decreasing energy (velocity and turbulence). E2 is interpreted as a large flood-induced turbidite either related to the formation of a hyperpycnal flow, where only the upper sequence was preserved because of strong erosion during the rising limb of the flood (Mulder et al., 2001a; Mulder et al., 2003), or to the development of a large homopycnal flow across the lake (Brodzikowski & Van Loon, 1991).

The formation of such exceptional flood deposits in Lake Bramant may result from the catastrophic drainage (i.e., outburst) of a temporary ice-contact lake or even a subglacial lake. The exceptional flood events E2 and E3, dated by varve counting (Guyard et al., subm) to AD 1904-1905 and AD 1908-1910, respectively, occurred when the St. Sorlin glacier was already retreating from its last advance following the end of the "Little Ice Age" (LIA), whereas the precise dating of the lowermost turbidite is still ongoing. Exceptional flood events in Lake Bramant could thus be linked to climatic oscillations through the outbursts of temporary ice contact lakes or subglacial lakes during warmer periods.

5. Conclusions

Various recent rapidly deposited layers were identified in high-altitude Lake Bramant sediments using several continuous high-resolution methods. The energy evolution of these different deposits is well distinguished by grain size statistical parameters and their trigger mechanisms were thus determined. The AD 1881 earthquake has triggered a slide that evolved into a slump. The recent hyperpycnal deposits (E2 and E3) are likely related to significant fluctuations of the St. Sorlin glacier following the end of the LIA. Nevertheless, as previously noted by Mulder et al. (2003) it can be difficult to distinguish flood-induced turbidites from hyperpycnites because erosion of the basal reverse grading sequence can occur during the rising limb of the flood or because the discharge and velocity during a high-magnitude flood are simply too important to allow sediment deposition. Ongoing complementary studies of Lake Blanc

Bramant sediments, the second proglacial lake of the chain and the main tributary of Lake Bramant, will allow a better understanding of the relationship between flood-induced turbidites and the fluctuations of the St. Sorlin glacier.

Acknowledgements

We thank Michel Vallon (LGGE) for fruitful discussions and Urs Gerber (ETH Zürich) for the core photographs. Thanks are also due to Fabien Arnaud and Olivier Magand for the radionuclide dating. Atle Nesje, Oyvind Lie and all the coring team from Bergen University (Norway) are sincerely acknowledged for the collection of piston core BRA03 and for the logistic support. This project was funded by the French Mountain Institute. This constitutes GEOTOP-UQAM-McGill contribution n° 2007-0017.

References

Arnaud, F., Lignier, V., Revel, M., Desmet, M., Beck, C., Pourchet, M., Charlet, F., Trenteseaux, A. & Tribovillard, N., 2002. Dating sediments from an alpine lake (Lake Anterne, NW Alps): influence of flood-events and gravity reworking on 210Pb vertical profile. *Terra Nova*, 14, 225-232.

Blott, S.J. & Pye, K., 2001. Gradistat: a grain size distribution and statistics package for the analysis of unconsolided sediments. *Earth Surf. Process. Landforms*, 26, 1237-1248.

Bouma, 1962. *Sedimentology of Some Flysch Deposits*. Elsevier, Amsterdam.

Brodzikowski, K. & Van Loon, A.J., 1991. Review of glacigenic sediments. *Development in Sedimentology*, 49, 688 p.

Chapron, E., Beck, C., Pourchet, M. & Deconinck, J-F., 1999. 1822 earthquake-triggered homogenite in Lake Le Bourget (NW Alps). *Terra Nova*, 11, 86-92.

Chapron, E., Ariztegui, D., Mulsow, S., Villarosa, G., Pino, M., Outes, V., Juvignié, E. & Crivelli, E., 2006. Impact of the 1960 major subduction earthquake in Northern Patagonia. *Quaternary International*, 158, 58-71 .

Croudace, I.W., Rindby, A. & Rothwell, R.G., 2006. ITRAX: description and evaluation of a new X-Ray core scanner. In R. G. Rothwell (Ed.), New Techniques in Sediment Core Analaysis. *Geol. Soc. Spec. Publ.* 267, pp. 51-63.

Doig, R., 1986. A method for determining the frequency of large-magnitude earthquake using lake sediments. *Canadian Journal of Earth Science*, 23, 930-937.

Guyard, H., Chapron, E, St-Onge, G., Anselmetti, F. S., Arnaud, F., Magand, O., Francus, P. & Mélières, M.A., in review. High-altitude varve records of abrupt environmental changes and mining activity over the last 4000 cal yr BP in the Western French Alps (Lake Bramant, Grandes Rousses Massif). *Quaternary Science Reviews.*

Locat, J. & Lee, H. J., 2002. Submarine landslides: advances and challenges. *Canadian Geotechnical Journal,* 39, 193-212.

Monecke, K., Anselmetti, F., Becker, A., Sturm, M. & Giardini, D., 2004. The record of historic earthquakes in lake sediments of Central Switzerland. *Tectonophysics*, 394, 21-40.

Mulder, T. & Cochonat, P., 1996. Classification of offshore mass movements. *Journal of Sedimentary research*, 66, 43-57.

Mulder, T., Migeon S., Savoye B. & Faugères J.C., 2001a. Inversely graded turbidite sequences in the deep Mediterranean: a record of deposits from flood-generated turbidity currents? *Geo-Marine Letters,* 21, 86-93.

Mulder, T., Weber, O., Anschutz, P., Jorissen, F. J. & Jouanneau, J.-M., 2001b. A few months-old storm generated turbidite deposited in the Capbreton Canyon (Bay of Biscay, SW France). *Geo-Marine Letters,* 21: 149-156.

Mulder, T., Syvitski, J.P.M., Migeon, S., Faugères, J-C. & Savoye, B., 2003. Marine hyperpycnal flows : initiation, behavior and related deposits. A review. *Marine and Petroleum Geology*, 20, 861-882.

Nomade, J., Chapron, E., Desmet, M., Reyss, J-L., Arnaud, F. & Ligner, V., 2005. Reconstructing historical seismicity from lake sediments (Lake Laffrey, Western Alps, France). *Terra Nova*, 17, 350-357.

Rothwell, R. G., Hoogakker, B., Thomson, J., Croudace, I. W. & Frenz, M., 2006. Turbidite emplacement on the southern Balearic Abyssal Plain (western Mediterranean Sea) during Marine Isotope Stages 1-3: an application of ITRAX XRF scanning of sediment cores to lithostratigraphic analysis. From Rothwell, R. G: *New techniques in sediment Core Analysis,* pp. 79-98. Geological Society, London.

Schnellmann, M., Anselmetti, F., Giardini, D., McKenzie, J.A. & Ward, S.N., 2002. Prehistoric earthquakes history revealed by lacustrine slump deposits. *Geology*, 30, 1131-1134.

Schneider, J-L., Pollet, N., Chapron, E., Wessels, M. & Wassmer, P., 2004. Signature of Rhine Valley sturzstrom dam failures in Holocene sediments of Lake Constance, Germany. *Sedimentary Geology,* 169, 75-91.

Sims, J. D., 1975. Determining earthquake recurrence intervals from deformational structures in young lacustrine sediments. *Tectonophysics*, 29, 141-152.

St-Onge, G. & Lajeunesse, P., this book. Flood-induced turbidites from northern Hudson Bay and Western Hudson strait: a two pulse record of Lake Agassiz final outburst flood?

St-Onge, G., Mulder, T., Piper, D.J.W., Hillaire-Marcel, C. & Stoner, J.S., 2004. Earthquake and flood induced turbidites on the Saguenay Fjord (Québec): a Holocene paleoseismicity record. *Quaternary Science Reviews,* 23, 283-294.

St-Onge, G., Mulder, T. & Francus, P, 2007. Continuous physical properties of cored marine sediments. In C. Hillaire-Marcel and A. de Vernal (Eds.), *Proxies in Late Cenozoic Paleoceanography (Developments in Marine Geology)*, pp. 65-101.

Strasser, M., Anselmetti, F.S., Fäh, D., Giardini, D. & Schnellmann, M., 2006, Magnitudes and source areas of large prehistoric northern Alpine earthquakes revealed by slope failures in lakes. *Geology* 34, 1005-1008.